Post-Cyclic Settlements of a Levee Structure on Organic Soil during Centrifuge Testing

Anne Lemnitzer
Department of Civil & Environmental Engineering, University of CA Irvine, Irvine, CA, USA
Riccardo Cappa
Simpson, Gumpertz & Heger Consulting Engineers, Irvine, CA, USA
Samuel Yniesta
Department of Civil, Geological and Mining Engineering, Ecole Polytechnique de Montréal, Montréal, Quebec, Canada
Jonathan P. Stewart
Department of Civil & Environmental Engineering, University of CA Los Angeles, Los Angeles, CA, USA
Scott J. Brandenberg
Department of Civil & Environmental Engineering, University of CA Los Angeles, Los Angeles, CA, USA

ABSTRACT
The seismic stability of embankment structures atop organic soils is controlled by the cyclic performance of the embankment fill and the response of the underlying foundation soil. Embankment failure can result from crest settlements (e.g., induced by liquefaction or immediate seismic deformations) combined with cyclic and post-cyclic volumetric strains in the soft foundation stratum due to primary consolidation and secondary compression. Centrifuge testing was executed to study the seismic interaction between a model levee made of modeling clay and the underlying peat. Subject to different loading conditions, the levee-peat response was evaluated using extensive model instrumentation consisting of pore pressure sensors, accelerometers, bender elements and external displacement transducers. Excess pore pressures developed in the peat during shaking were analyzed to compute secondary compression settlement rates due to cyclic straining. Post-seismic rate increases in secondary compression settlements were documented directly underneath the levee and in the free field arrays of the model, respectively. This suggests a strong potential hazard for accelerated long term crest settlements (i.e. reduction of freeboard) following seismic events, in particular, for areas with minimal pre-earthquake secondary settlement rates. Experimental settlements are compared with results obtained through a nonlinear consolidation software package that follows an implicit finite difference formulation set to include the secondary compression deformation of soft soils concurrently with primary consolidation. Results indicate that secondary compression may control settlements in peat; therefore, the influence of cyclic straining on secondary compression is an important consideration in design and retrofit of current/future embankment structures.

1 INTRODUCTION

Over the past 20 years, the consolidation behavior of peat has been actively researched via experimental and analytical studies, (e.g., Fox and Edil 1992, Mesri et al. 1997, Mesri and Ajlouni 2007, and Kazemian et al. 2011). These studies indicate that the secondary compression behavior of peat is significant, and often dominates long-term volumetric strains. The dynamic properties of peat have also been studied by various researchers, e.g., Boulanger et al. 1998, Kramer 2000, Wehling et al. 2003, and Tokimatsu and Sekiguchi 2007, who focused on the effects of loading frequency, cyclic degradation, stress history, etc. and proposed relationships for modulus reduction and damping. Egawa et al. (2004) investigated the behavior of embankment structures on soft peat via centrifuge experiments, with a specific focus on the effects of model geometry and input motions on the accelerations and strains developed in the foundation soil, however; Egawa et al. did not describe the volumetric changes and pore pressures generated in the peat itself.

For levees structures located in the Sacramento/San Joaquin Delta in California, global instability resulting from crest settlements (e.g., induced by liquefaction or immediate seismic deformations) combined with cyclic and post-cyclic volumetric changes of the soft foundation stratum (e.g. short and long term reconsolidation) characterizes the most important potential for embankment failure. Levee structures impounding water could breach or experience significant loss of freeboard and consequently flood the protected Delta "islands", disrupting delivery of fresh water to urban and agricultural users in central and southern California. In this paper, we focus on the influence of cyclic loading on the primary and secondary consolidation settlements of the organic foundation soil. Shafiee et al. (2015) studied the influence of cyclic loading on post-cyclic volume change behavior of peat located in the Sacramento-San Joaquin Delta via laboratory testing. They discovered that the peat generates small excess pore pressure during cyclic loading when shear strains exceed about 1%. Perhaps more importantly, they found that cyclic loading may partially or fully reset secondary compression behavior, potentially accelerating settlement of levees that survive strong shaking. The secondary compression increased when cyclic shear strains exceeded about 0.1%, and the

rate increased as shear strain amplitude and number of cycles increased.

Cappa et al. (2017) further studied the development of strains and pore pressures developed during centrifuge testing of model levees resting on peat and subject to various ground motions. Shear strains as high as 7% were mobilized in the peat for ground motions with peak base accelerations of 0.52g. Cappa et al. observed the shear strain threshold beyond which excess pore pressures are generated in the peat to be near 1.0%. This strain level is consistent with the direct simple shear laboratory studies. The maximum residual excess pore pressure ratio recorded during the experimental investigation was 0.2. Similar agreement is observed with general shear strain ranges and excess pore pressures for peats from the Delta region tested in triaxial studies by Wehling et al. (2003). These residual excess pore pressures are potentially very important due to the post-earthquake settlements that arise from reconsolidation. Although the residual excess pore pressure ratios are modest, the compressibility of the peat is very high and the post-cyclic volumetric strains have potential to be significant.

The objective of this paper is to focus on the effect of seismic loading on the post-cyclic volumetric strain of peat underlying a levee tested in a centrifuge modeling program. Upon a brief review of the experimental research program, including a compact description of the model and material parameters, we will present strain and settlement recordings in the peat and narrow the discussion towards pre-and post-cyclic settlement rates. Experimental observations will then be compared with a recently developed consolidation software package by Brandenberg (2017).

2 REVIEW OF CENTRIFUGE TESTING PROGRAM

The experimental investigation was conducted at the 9m radius geotechnical centrifuge facility located at the University of California, Davis. The specific experiment selected for discussion consisted of a non-liquefiable levee made of modeling clay placed atop a layer of peat to study the settlement response of the organic foundation soil. In a later phase, the clayey levee structure was replaced with a saturated sandy levee to study the liquefaction potential of the levee itself. Experiment reports, test data and media documentation of all investigations associated with the levee project can be downloaded from the NEES repository under: (https://nees.org/warehouse/project/1161) and are described in detail by Lemnitzer et al. 2015.

2.1 Test Setup, Instrumentation and Loading

The prototype model consists of a 5.1m thick levee overlying 6.1m of peat over 8.6m of dense coarse sand. The levee crest and base widths are 10.3 m and 30 m, respectively, and side slopes are 2:1. The model was instrumented with accelerometers, linear potentiometers, pore pressure transducers and bender elements to capture the static (slow data, e.g. consolidation process) and dynamic (fast data, e.g. ground motion) response of the system. Sensors are omitted from Figure 1, but the sensor layout can be found in the data report for the experiment. Testing was conducted at 57g. Following spin-up, each model was allowed to consolidate until excess pore pressures were essentially zero (approximately one hour) prior to applying the ground motions. Table 1 presents the sequence of motions applied to the base of the model during the clay-levee phase. For the Kobe earthquake, a scaled version of record PRI090/KP4090 was used and for the Loma Prieta motion record LGP090 was implemented. Please note that the input ground motions and actual container motions vary. Figure 2 depicts a photograph of the experiment in flight right before the application of the ground motions. Dashed lines in Figure 1 indicate the initial position of the levee and peat prior to spinning. During spin up and primary consolidation at 57g, the peat in the center levee array settled approximately 4.16 m in prototype scale,. This settlement corresponds to 40% vertical strain. The free field peat settled about 2.0 m in prototype scale, which corresponds to 21% vertical strain.

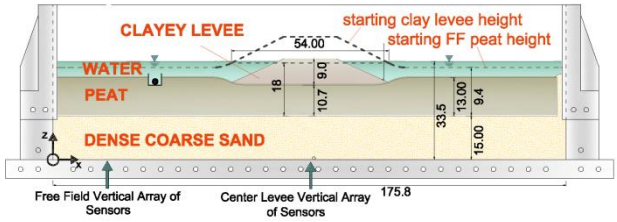

Figure 1. Setup of the clay-levee experiment following primary consolidation (all dimensions in prototype scale).

Table 1: Ground motion sequence. PBA = peak base acceleration. Nomenclature in accordance with Lemnitzer et al. 2015 & the NEES data repository.

Exp #	Trial #	Input Motion	PBA[g] @ base prototype scale
14	2	Step Wave 1	0.006
14	3	Sine Sweep 1	0.018
14	4	Large Kobe	0.56
14	5	Large Loma Prieta	0.421
14	6	Medium Kobe	0.288
14	7	Small Kobe	0.125

2.2 Material Properties

The dense layer of coarse sand (Figure 1) was placed via dry pluviation at the bottom of the container. The material had a unit weight of 20.2 kN/m^3 and an approximate relative density D_R of 90%. This layer was added to simulate a common stratigraphy encountered in the Delta and to provide a drainage stratum for the peat during consolidation.

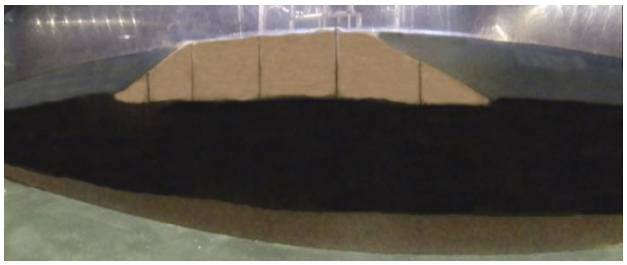

Figure 2. Photograph of the clay levee model in flight prior to the application of ground motions.

The peat was excavated from a depth of 2-3 m at Sherman Island in the Delta and transported to the centrifuge facility. During storage and handling, the peat was kept submerged to avoid desiccation. The peat was placed into the model as a slurry, and lightly consolidated beneath a thin layer of sand. The virgin peat contained long fibers and clusters that were removed prior to placement in the centrifuge to obtain a more homogeneous material suitable for the centrifuge model. The clayey levee was constructed using oil-based modeling clay with a unit weight of 18 kN/m^3. Shear wave velocities of the different materials were measured via bender elements placed in the respective layers. The free-field shear wave velocities of the peat varied between 5 and 14 m/sec across the layer height. The shear wave velocity of the peat underneath the levee was measured to be 26-28 m/s. Table 2 reports the material characteristics of the processed peat determined via laboratory testing.

Table 2: Characteristics of the peat

Property	Measured
Initial water content, w	670-870%
Average organic content, OC	69%
Initial total unit weight, γ_t	10.28 – 10.41 kN/m^3
Specific Gravity of Solids, Gs	1.79
Initial Void Ratio, e_0	12 – 15.5
Ave. Compression Index Odometer, Cc	3.8

3 DATA ANALYSIS

3.1. Measured Settlements using Slow Data Recordings

The large Kobe motion (Table 1) was selected for a detailed settlement analysis because it generated the largest pore pressure in the peat. Pore pressure and displacement time histories using the sensors shown in Figure 3 are plotted for a selected time range in Figure 4. The time frame in Figure 4 includes the model spin-up to the target acceleration, the system check through step and sin waves (not visible in the time history plot) and the large Kobe ground motion. The dynamic characteristics of the Kobe motion are barely visible in the slow data shown in Figure 4 because the event occurred so quickly compared to the time scale; each motion is essentially an instantaneous event as plotted in Figure 4. A close up of the Kobe motion is therefore depicted in Figure 5.

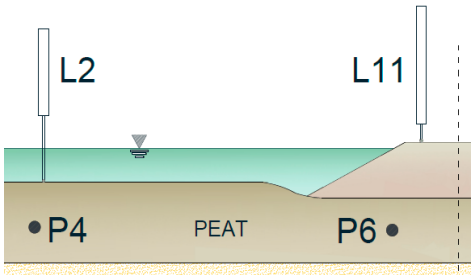

Figure 3: Sensor instrumentation used for time-history analyses: free-field and center-levee pore pressure (P4/P6) and settlement sensors (L2/L11), respectively.

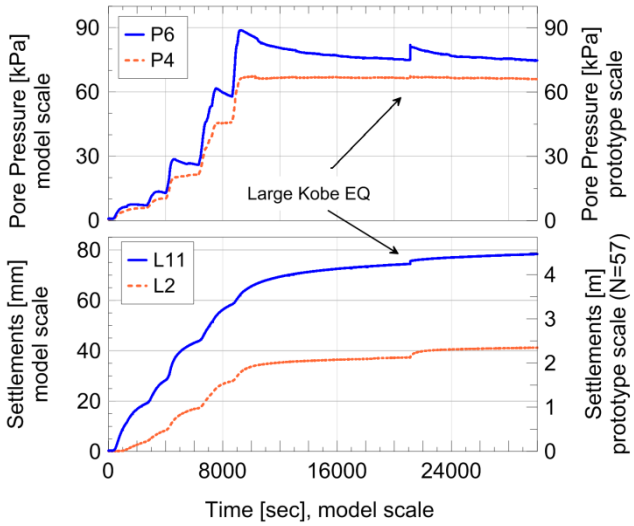

Figure 4: Pore pressure and settlement histories during spin up and application of the Large Kobe Motion

Significantly larger settlement occurred at sensor L11 (center levee) than for L2 (free field) during spin-up due to the higher vertical effective pressure beneath the levee (approx. 50 kPa at center of peat layer) compared with the free field (approx. 3 kPa at center of peat layer). A zoomed-in version of the time history record surrounding the large Kobe motion is shown in Figure 5. The Kobe motion generated excess pore pressures of about 6.93 kPa and 1.1 kPa in the peat beneath the center of the levee and in the free-field. The total prototype settlements recorded during and after the Large Kobe motion until the next ground motion was applied consisted of approximately 25.6 cm and 22.9 cm beneath the levee crest and in the free-field, respectively. The settlement is divided among the following components: co-seismic settlements of approximately 6.3 cm and 2.9 cm, and post-seismic settlements (i.e., primary consolidation and secondary compression) of 19.3 and 20.0 cm underneath the levee and free field respectively. Figures 4 and 5

illustrate that pore pressures underneath the levee (P6) required much more time to reach pre-loading levels. Following earthquake application, the model was allowed to enter the secondary compression stage before applying the next ground motion.

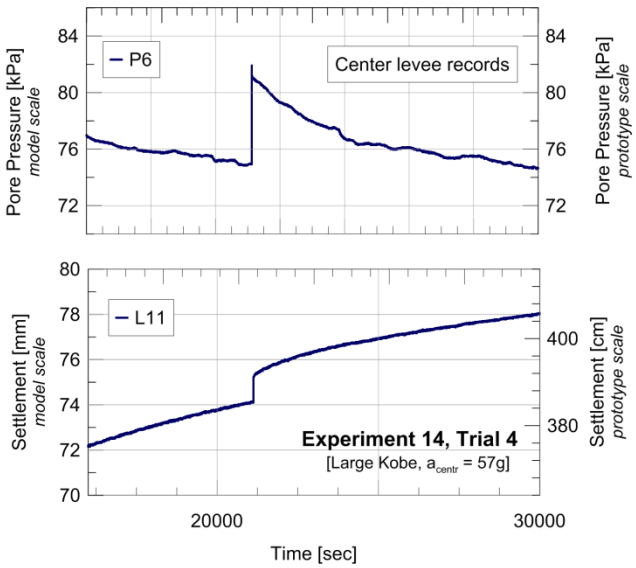

Figure 5: Co- and post seismic pore pressure and settlement records during the large Kobe motion in the center levee array

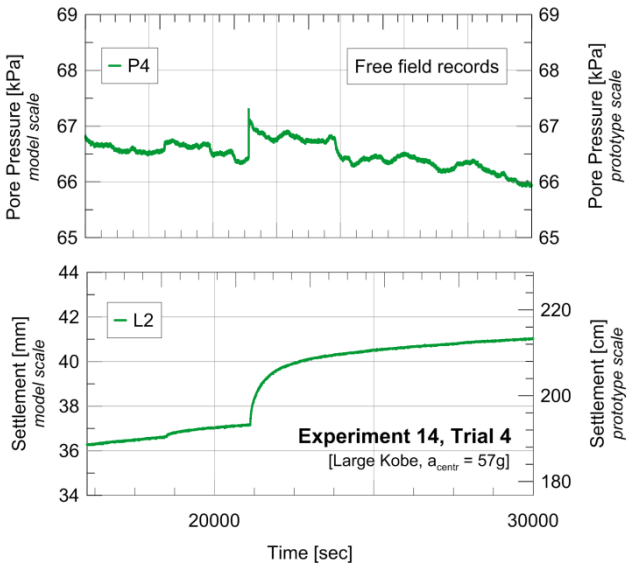

Figure 6: Co- and post seismic pore pressure and settlement records during the large Kobe motion in the free field

4. NUMERICAL SETTLEMENT STUDIES

The traditional approach to primary consolidation and secondary compression assumes that the two mechanisms occur in distinct regions of time, with primary consolidation occurring from time = 0 (corresponding to the application of loading) until t_p, and secondary compression occurring after t_p. This approach is problematic because in reality, some secondary compression occurs simultaneously with primary consolidation. Thick layers that take longer to consolidate would exhibit more secondary compression than thinner layers that consolidate more quickly; a concept identified by Bjerrum (1967) in his "time line" theory. Furthermore, the benchtop clock provides an arbitrary time reference that is not tied to the soil state. Brandenberg (2017) formulated an alternative approach in which the secondary compression strain rate is a function of position in e-log σ_v' space relative to a reference secondary compression line (RSCL). Modeling secondary compression in this manner enables both mechanisms to occur simultaneously. The nonlinear nonlinear 1D implicit finite difference code is publically available as a JavaScript Web-based application called "iConsol.js" at: www.uclageo.com/Consolidation/

Within this approach, the secondary compression strain rate decreases as the void ratio decreases and the current stress state moves down relative to the RSCL, which is assumed to be stationary. This is inconsistent with the experimental observation that the secondary compression settlement rate increased following cyclic loading. One approach for modeling the increase in settlement rate is to shift the RSCL downward from its current position toward the current point in stress-space. Assuming the RSCL is initially coincident with the normal consolidation line, shifting the RSCL all the way down to the current stress point would constitute a full reset of secondary compression behavior, resulting in the strain rate being identical to that for a normally consolidated soil. The amount of downward shift can be represented by a secondary compression reset index, I_R, such that $I_R = 0$ corresponds to no secondary compression reset, and $I_R = 1$ corresponds to full reset.

Shafiee (2016) presented equations for residual excess pore pressure ratio (i.e. the pore pressure ratio at the end of cyclic loading), r_{ur}, and I_R as functions of cyclic strain amplitude, γ_c, number of cycles, N, overconsolidation ratio, OCR, organic content, OC, and static shear stress ratio, $\alpha = \tau_s/\sigma_{vo}'$, as indicated in Equations 1 and 2.

$$r_{u,r} = 0.316(\gamma_c - \gamma_{tp})^{0.619} \cdot N^{0.187} \cdot OCR^{-0.477} \cdot OC^{-0.499} \quad [1]$$

$$I_R = \gamma_c^{0.219} N^{0.261} \left(0.899\alpha + 0.939\right) \times \left(-0.043OC + 0.300\right) \left(0.192 \frac{\sigma_{vo}'}{p_a}\right) \times \left(0.009OCR + 0.980\right) \quad [2]$$

In Eq. (2), p_a refers to the atmospheric pressure (i.e., 101.3 kPa) and γ_{tp} the strain threshold after which strain level pore pressure generation is to be expected during a cyclic motion. To obtain an objective comparison between settlements measured in the centrifuge models and estimations using iConsol.js, the input parameters for

compressibility, secondary compression, and permeability were selected from laboratory tests on peats reported by Shafiee (2016). Specifically, the normal consolidation line parameters were based on the e-log σ_v' relationships observed during consolidation testing in the laboratory. Permeability parameters were estimated from falling head tests. Secondary compression properties were obtained from the consolidation test. By using the soil properties as reported by Shafiee who tested a wide range of peats to develop the regression formulations as described above, we are able to perform the settlement predictions as "blind predictions". Therefore input parameters depicted in Figure 7 reflect the peat tested by Shafiee (2016) and Shafiee et al. 2013 that is closest to our peat. We found this selection more meaningful, as a design engineers in "real-world" design scenarios would only have a limited amount of information available to conduct such analyses.

The secondary compression reset was modeled using the "advanced" setting in the input window by reducing the value of $e_{c\alpha,ref}$ by an amount proportional to I_R multiplied by the difference in void ratio between the RSCL and the stress condition prior to imposing the Kobe motion. The overconsolidation ratio was computed based on the measured settlement at the time of application of the Kobe motion. Figure 8 shows a screen shot of the input parameters available in the iConsol software package.

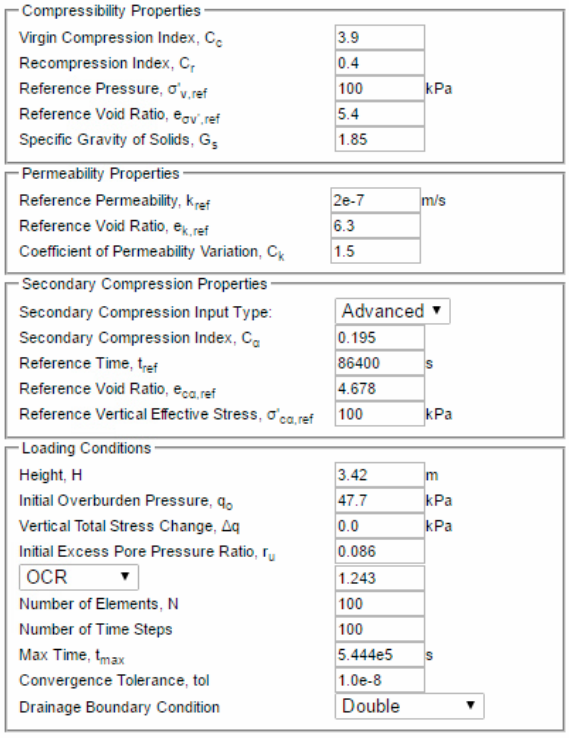

Figure 7: Input parameters in the consolidation software based on peat laboratory results and measured strain histories (screen shot of analysis run that includes secondary compression reset)

To compute values of I_R and $r_{u,r}$, the cyclic shear strain must be known. These values were measured from accelerometers embedded in the peat underneath the levee as described in detail by Cappa et al. 2017. The strain path in the peat beneath the levee is more complicated than that used in Shafiee's direct simple shear program. To account for the more complex strain history, components of the Cauchy strain tensor $\varepsilon_{xx}, \varepsilon_{zz}, \gamma_{xz}$ are computed first from measured dynamic displacements, and subsequently used to compute a direct simple shear deviatoric strain invariant, $\gamma_{DSS,eq}$ defined in Eq. 3. Figure 8 shows the resulting direct simple shear strain history during the application of the Large Kobe motion.

$$\gamma_{DSS,eq} = \sqrt{\frac{2}{3}} \cdot \sqrt{\left(\varepsilon_{xx}\right)^2 + \left(-\varepsilon_{zz}\right)^2 + \left(\varepsilon_{zz} - \varepsilon_{xx}\right)^2 + 6 \cdot \left(\frac{\gamma_{xz}}{2}\right)^2} \quad [3]$$

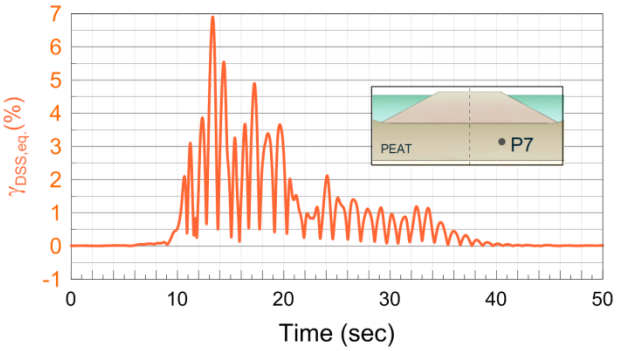

Figure 8: Direct simple shear time history for the location of sensor P7 during the Large Kobe motion.

In order to use Eqs. 1 and 2, an equivalent number of uniform cycles (N) and corresponding shear strain amplitude γ_c must be computed from the irregular $\gamma_{DSS,eq}$ time series. This is accomplished by counting strain cycles, and weighting them in proportion to the strain amplitude, in a manner that is similar to procedures commonly utilized in liquefaction triggering analyses. The number of cycles was set to 15, and the equivalent value of γ_c was computed from the broadband strain history.

Figure 9 depicts a comparison of recorded and predicted settlements in the center levee array following the Large Kobe earthquake motion. Three different predictions were performed: (1) primary consolidation only (i.e., with C_α = 0), (2) primary consolidation and secondary compression with no reset (i.e., I_R = 0), and (3) primary consolidation and secondary compression accounting for reset induced by the deviatoric strain history mobilized during the Kobe motion. The comparison shows clearly that secondary compression is the primary source of settlement, with primary consolidation contributing a relatively small fraction.

Primary consolidation is small for this problem because the excess pore pressure ratio was only 0.086 (as calculated by Eq. 1). Furthermore, settlement is under-predicted when secondary compression reset is ignored. Only a correct inclusion of the reset mechanism (i.e. the integration of the accelerated secondary compression rate after seismic loading) is able to capture the measured settlements and yield an accurate prediction of the results.

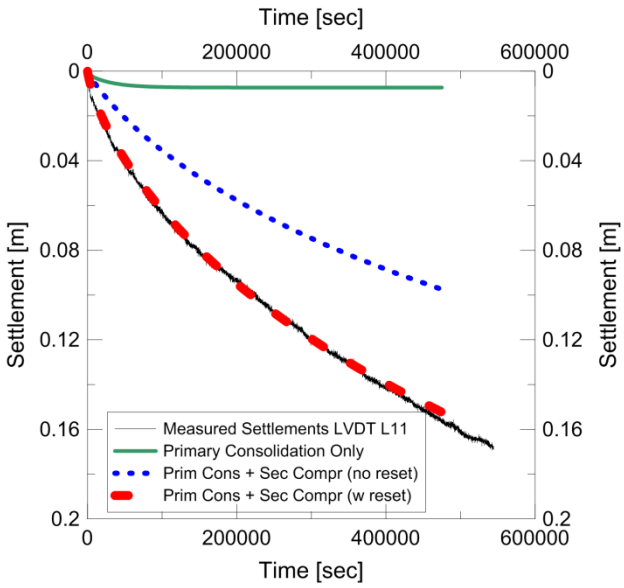

Figure 9: Comparison of measured post-cyclic settlements with predictions using the iConsol software package by Brandenberg (2017).

5 SUMMARY AND CONCLUSIONS

A large scale 9m radius centrifuge test, conducted at the NEES facility at UC Davis, was analyzed to gain insight into the complex soil-structure-interaction (SSI) mechanism of levees located on soft peaty soils. This paper focused on the cyclic and post-cyclic volumetric change of the peat material and its contribution to the seismic demand on the levee structures. Rate increases in secondary compression settlements of 18% and 52% were documented in the center levee and free field arrays of the model, respectively. This suggests a strong potential hazard for accelerated long term crest settlements (i.e. reduction of freeboard) following seismic events, in particular for areas with minimal pre-earthquake secondary settlement rates. Post-cyclic settlements were compared with a 1D nonlinear implicit finite difference code developed by Brandenberg (2017) which enables both settlement mechanisms (i.e. primary consolidation and secondary compression) to occur simultaneously. Input parameters were selected based on laboratory testing of the centrifuge peat, and strain histories measured during the ground motion application were used to estimate excess pore pressure ratio and secondary compression reset based on laboratory test results by Shafiee (2016). Comparisons between measured and predicted settlements show that (1) secondary compression is the dominant settlement mechanism, with a relatively small contribution from primary consolidation, and (2) secondary compression reset had to be included to provide a good match to measured settlements; excluding secondary compression reset resulted in an under-prediction.

6 ACKNOWLEDGEMENTS

This research was funded by the National Science Foundation under grant No. CMMI 1208170. Any opinions, findings, and conclusions or recommendations expressed in this material are those of the author(s) and do not necessarily reflect the views of the National Science Foundation. The writers would like to acknowledge the valuable assistance of the UC Davis centrifuge team.

7 REFERENCES

Bjerrum, L. 1967. “Engineering geology of Norwegian normally consolidated marine clays as related to settlements of buildings.” Geotechnique, 17(2), 83–118.

Boulanger, R.W., Arulnathan, R., Harder, L.F.J., Torres, R.A., and Driller, M.W. 1998. Dynamic Properties of Sherman Island Peat, *Journal of Geotechnical and Geoenviromental Engineering*, ASCE, 124(1): 12-20.

Brandenberg, S.J. 2017. iConsol.js: JavaScript Implicit Finite-Difference Code for Nonlinear Consolidation and Secondary Compression. *International Journal of mechanics*,ASCE http://dx.doi.org/10.1061/(ASCE)GM.1943-5622.0000843

Cappa, R., Brandenberg, S.J. and Lemnitzer, A. 2017. Strains and pore pressures generated during cyclic loading of embankments on organic soil. *Journal of Geotechnical and Geoenviromental Engineering*, ASCE (accepted).

Egawa, T., Nishimoto, S. and Tomisawa, K. 2004. An Experimental Study on the Seismic Behavior of Embankments on Peaty Soft Ground Through Centrifuge Model Tests, *13th World Conference on Earthquake Engineering*, Paper No. 36.

Fox, P.J., and Edil, T.B. 1992. Cα/Cc concept applied to compression of peat, *Journal of Geotechnical Engineering*, ASCE, 118(8): 1256-1263.

Kazemian, S., Huat, B.B.K., Prasad, A. and Barghchi, M. 2011. A State of Art Review of Peat: Geotechnical Engineering Perspective, *International Journal of the Physical Science*, 6 (8): 1974-1981.

Kramer, S.L. 2000. Dynamic Response of Mercer Slough Peat, *Journal of Geotechnical and Geoenviromental Engineering*, ASCE, 126(6): 504-510.

Lemnitzer, A., Cappa, R., Yniesta, S. and Brandenberg, S.J. (2015) “Centrifuge Testing of Model Levees atop Peaty Soil: Experimental Data”, *Earthquake Spectra*, http://dx.doi.org/10.1193/032715EQS048

Mesri, G., Stark, T.D., Ajlouni, M.A. and Chen, C.S. 1997. Secondary Compression of Peat with or without Surcharging, *Journal of Geotechnical and Geoenvironmental Engineering*, ASCE, 123(5): 411-421.

Mesri, G. and Ajlouni, M.A. 2007. Engineering Properties of Fibrous Peat, *Journal of Geotechnical and Geoenvironmental Engineering,* 133(7): 850-866.

Shafiee, A. 2016. Cyclic and post-cyclic behavior of Sherman Island Peat, *PhD Dissertation*, University of California, Los Angeles.

Shafiee, A., Brandenberg, S.J., and Stewart, J.P., 2013. Laboratory investigation of the pre-and post-cyclic volume change properties of Sherman Island peat, *GeoCongress,* San Diego, CA, Publication No.231

Shafiee, A., Stewart, J.P., and Brandenberg, S.J. 2015. Reset of secondary compression clock for peat by cyclic straining*, Journal of Geotechnical and Geoenvironmental Engineering*, ASCE, 141(3).

Tokimatsu, K. and Sekiguchi, T. 2007. *Effects of Dynamic Properties of Peat on Strong Ground Motions During 2004 Mid Niigata Prefecture Earthquake, 4th International Conference on Earthquake Geotechnical Engineering*, Paper No. 1531.

Wehling, T.M., R.W. Boulanger, R. Arulnathan, L.F. Harder and M.W. Driller 2003. Nonlinear dynamic properties of a fibrous organic soil, *Journal of Geotechnical and Geoenvironmental Engineering*, ASCE, 129(10): 929-939.